

Monte Carlo study of three-dimensional-to-one-dimensional crossover in the Ising model

Tom Graim and D. P. Landau

Department of Physics and Astronomy, University of Georgia, Athens, Georgia 30602

(Received 25 November 1980)

Monte Carlo calculations have been used to study the behavior of a simple cubic spin- $\frac{1}{2}$  Ising model with spatially anisotropic nearest-neighbor coupling. The interaction in the  $x$  and  $y$  directions, which is equal to  $(J_{\perp})$ , was systematically decreased compared to that in the  $z$  direction  $(J_{\parallel})$ , and results were obtained for values of  $\Delta = J_{\perp}/J_{\parallel}$  as small as 0.003. For small  $\Delta$  the system behaves like a one-dimensional Ising chain at high temperature before undergoing a low-temperature transition to a three-dimensionally ordered state. We find that the asymptotic ( $\Delta \rightarrow 0$ ) variation of  $T_c$  is accurate over a surprisingly wide range of  $\Delta$ .

I. INTRODUCTION

Three-dimensional (3D) Ising models and (pseudo-) Ising physical systems have been studied extensively.<sup>1,2</sup> Since an increasing number of pseudo-1D physical systems are being discovered and studied,<sup>3</sup> the behavior of Ising models with spatially anisotropic interactions is gaining significance. In this paper we shall focus our attention on a system of  $S = \frac{1}{2}$  Ising spins arrayed on a simple cubic lattice and interacting with the Hamiltonian

$$\mathcal{H} = -J_{\parallel} \sum_{zNN} \sigma_i \sigma_j - J_{\perp} \sum_{x,yNN} \sigma_i \sigma_k, \tag{1}$$

where  $\sigma_i, \sigma_j, \sigma_k = \pm 1$ ,  $J_z$  is the coupling between nearest-neighbor (NN) spins in the  $z$  direction and  $J_{\perp}$  is the interaction between NN spins in the  $x$  and  $y$  directions. In the limit that the interaction ratio  $\Delta = J_{\perp}/J_{\parallel} \rightarrow 1$  the model becomes a simple, spatially isotropic 3D model; but as  $\Delta \rightarrow 0$  the system separates into a collection of noninteracting Ising chains which show no long-range order. This model has been studied<sup>4</sup> using a modified mean-field theory in which the intrachain coupling  $J_{\parallel}$  is treated exactly and the interactions between chains  $J_{\perp}$  are considered using mean-field theory. This method predicts a variation of the critical temperature for small  $\Delta$  given by

$$kT_c = 8J_{\perp} \exp(2J_{\parallel}/kT_c). \tag{2}$$

Simple universality arguments predict that the critical behavior should not change with  $\Delta$  and indeed series expansions studies<sup>5,6</sup> suggest that the critical exponents are independent of  $\Delta$ . The asymptotic variation of the critical temperature as  $\Delta \rightarrow 0$  has been determined<sup>7</sup>

$$\frac{kT_c}{J_{\parallel}} = 2 \left\{ \ln \left( \frac{1}{\Delta} \right) - \left\{ \ln \left[ \ln \left( \frac{1}{\Delta} \right) \right] + \dots \right\} \right\}^{-1} \tag{3}$$

but the range of validity of Eq. (3) is unclear. This result does show however that the modified mean-field treatment described earlier is seriously in error except in the limit where  $\Delta \rightarrow 0$ . In order to more fully understand the crossover from 3D to 1D behavior as  $\Delta \rightarrow 0$ , we have used computer simulations to study a simple cubic Ising model with the Hamiltonian given in Eq. (1) on  $L \times L \times pL$  lattices with periodic boundary conditions. As part of this study we shall pay attention to the effects of both lattice size and lattice shape (i.e., variation with  $p$ ). Results are presented for  $1.0 \geq \Delta \geq 0.003$ .

In the next section we shall describe the methods used and in Sec. III we shall present typical data. In Sec. IV we shall analyze finite size and shape effects and shall extract the behavior expected for infinite systems.

II. METHODS

A. "Standard" Monte Carlo technique

Most of our data were obtained using a simple equal-time-step importance sampling Monte Carlo method.<sup>8</sup> Successive states are generated by moving from site to site and flipping spins with a probability  $\rho$ :

$$\rho = \begin{cases} \exp(-\Delta E/kT), & \Delta E > 0 \\ 1, & \Delta E \leq 0 \end{cases} \tag{4a}$$

$$\tag{4b}$$

where  $\Delta E$  is the change in energy caused by the spin-flip. For a system of  $N$  sites we define the time unit 1 Monte Carlo step/spin (MCS) as  $N$  "microtrials" or spin-flip attempts. Estimates for thermodynamic parameters are made by averaging over the values obtained at the end of each MCS. Typically 1000-2000 MCS were retained for computing averages for each data point and each point was then re-

peated at least once using a different starting configuration. A more extensive description of the method has been published elsewhere<sup>8</sup> and the reader is referred there for further details.

### B. “*n*-fold way” Monte Carlo technique

At very low temperatures the probability of flipping a spin using the standard technique described in the previous section becomes extremely small. At these temperatures the evolution of the system becomes so slow as to be uneconomical; i.e., the number of MCS required becomes prohibitive. As we shall see in Sec. III the region of interest for small  $\Delta$  (near the phase transition) is  $kT \ll J$ . In order to overcome the time problem we developed an alternative program using a continuous-time method (the *n*-fold way) developed by Bortz, Kalos, and Lebowitz.<sup>9</sup> Rather than picking a site and then carrying out spin-flip attempts as in the standard method, this new method flips a spin at each trial and determines instead the time which elapsed since the previous flip. Since every spin-flip trial is successful this new method is clearly more efficient at low temperatures. This method is practical for an Ising model since there are a very limited number of possible spin environments (i.e., number of nearest neighbors which are up or down). Our program is slightly more complicated than that described by Bortz *et al.*<sup>9</sup> since we have two kinds of nearest-neighbors leading to a total of  $n = 30$  classes of spins plus environment. The probability of flipping any spin in a class is identical and equal to

$$p_i = \begin{cases} N_i \exp(-\Delta E/kT), & \Delta E > 0 \\ N_i, & \Delta E \leq 0 \end{cases} \quad (5a)$$

$$(5b)$$

where  $N_i$  is the number of spins in class  $i$  and total probability is

$$Q = \sum_{i=1}^{i=30} p_i \quad (6)$$

A random number between zero and  $Q$  is used to decide which class of spin shall be flipped and then a second random number is generated to determine which of the spins in the class shall be flipped. The lifetime of the previous state (i.e., before the spin was flipped) is then computed:

$$\Delta t = -\frac{\tau}{Q} \ln R \quad (7)$$

where  $R$  is a random number between zero and 1 and  $\tau$  is the average time between attempted spin flips (i.e., 1 microtrial in the standard method). Note that the time interval depends explicitly on  $Q$  which must be redetermined after each spin flip. At low temperatures  $Q$  becomes small and  $\Delta t$  will generally be large. In fact at very low temperatures the *n*-fold way method becomes orders of magnitude more efficient

than the standard method, but some of the advantage is lost because the increased complexity increases the running time for the program. For  $\Delta = 0.01$  with a  $4 \times 4 \times 24$  lattice the net improvement obtained using the *n*-fold way was 8.1 at  $T_c$ , 300 at  $\frac{2}{3} T_c$ , and  $1.3 \times 10^4$  at  $T_c/2$ . (More extensive information on this method is available in Refs. 9 and 10.) This new technique was only partially successful for the following reason: for very small  $\Delta$  the only flips which are likely at low temperatures are single spins overturned in an ordered chain. When a spin is overturned from the completely ordered state it forms a class by itself and is very likely to reflip before any of its intra-chain neighbors overturn. This problem could also lead to trapping an entire chain in a metastable state where all spins in one chain were reversed with respect to all other spins in the system. In any case the method was helpful in obtaining data for  $\Delta = 0.003$  and 0.01.

### C. Finite-size scaling theory

The behavior of a finite  $L \times L \times L$  system with periodic boundary conditions can be related to the infinite lattice properties by finite-size scaling theory.<sup>11</sup> The pseudocritical temperature  $T_c^L$  is given by

$$T_c^L = T_c + aL^{-1/\nu} \quad (8)$$

where  $T_c$  is the infinite lattice critical temperature and  $\nu$  is the infinite lattice exponent. Bulk properties are described by the scaled variable  $x = tL^{1/\nu}$  where  $t = |1 - T/T_c|$

$$M = L^{-\beta/\nu} \bar{X}(x) \quad (9a)$$

$$\chi T = L^{\gamma/\nu} \bar{Y}(x) \quad (9b)$$

$$C/R = L^{\alpha/\nu} \bar{Z}(x) + b \quad (9c)$$

where in the limit  $x \rightarrow \infty$  (with  $t$  small) the usual power laws must be retrieved:

$$M = Bt^\beta \quad (10a)$$

$$\chi T = \begin{cases} E^+ t^{-\gamma}, & T < T_c \\ E^- t^{-\gamma}, & T > T_c \end{cases} \quad (10b)$$

$$(10c)$$

$$C/R = A^\pm t^{-\alpha} + b \quad (10d)$$

Comparison of Eqs. (9) and (10) shows that the scaling functions must have simple asymptotic forms, e.g.,  $\bar{X}(x) \rightarrow x^\beta$ . If the lattice is no longer symmetric, e.g.,  $L \times L \times pL$  with  $p \neq 1$ , or if the correlation length grows unequally in different directions, i.e.,  $\Delta \neq 1$ , the scaling variable may need to be modi-

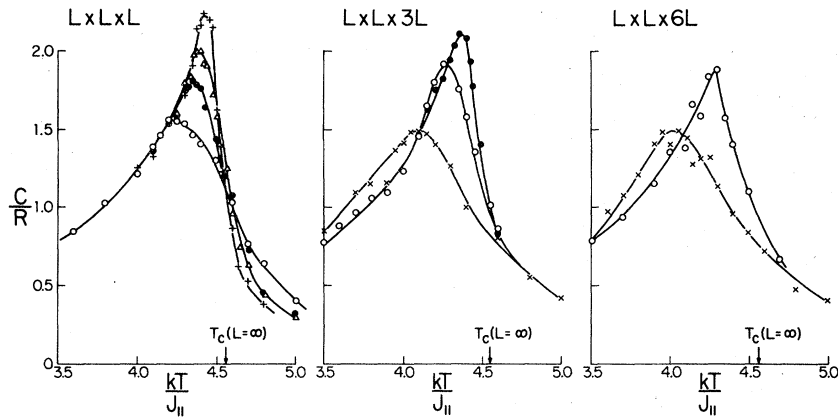


FIG. 1. Temperature dependence of the specific heat for different sample shapes for  $\Delta = 1.0$ . Data are shown for:  $L = 4, x$ ;  $L = 6, \circ$ ;  $L = 8, \bullet$ ;  $L = 10, \Delta$ ;  $L = 14, +$ .

fied. We have retained Eq. (9) but have considered several phenomenological possibilities for replacing  $L$  by an effective value<sup>11</sup>:

$$\bar{L} = \sqrt{3} \left[ 2 \left( \frac{\Delta}{L} \right)^2 + \left( \frac{1}{pL} \right)^2 \right]^{-1/2}, \quad (11a)$$

$$\bar{L}^{-1} = \frac{1}{3} \left( \frac{2}{L} + \frac{1}{pL} \right). \quad (11b)$$

In fact it is probable that Eq. (9) needs to be modified but it is unlikely that our data are sufficiently accurate to provide a valid test of alternative expressions.

### III. RESULTS

#### A. $\Delta = 1.0$

Both the  $L \times L \times L$  finite-lattice behavior as well as the infinite-lattice properties are well known<sup>12</sup> for the case of spatially isotropic interactions, i.e.,  $\Delta = 1.0$ . Previous studies of  $L \times M$  Ising square lattices<sup>13</sup> showed that the finite-size effects were strongly dependent on the lattice shape. We therefore decided to extend the earlier Monte Carlo study<sup>12</sup> of  $L \times L \times L$  simple cubic Ising lattices to include elongated finite samples to identify the dependence of properties on lattice shape. For this reason we carried out Monte Carlo calculations for  $L \times L \times pL$  lattices where  $p$  was an integer between 1 and 6. Typical specific-heat data are shown in Fig. 1. Note that the total number of sites in a lattice is  $N = pL^3$ ; hence for  $L = 6$  with  $p = 6$  the lattice ( $N = 1296$ ) is actually slightly larger than for  $L = 10$  with  $p = 1$  ( $N = 1000$ ). As  $p$  increases, with  $N$  held fixed, the finite-size effects become more pronounced both in terms of the rounding of the specific-heat peak as

well as the shift of the peak position to lower temperature.

In Fig. 2 we show the behavior of the spontaneous magnetization for two different sample shapes:  $p = 1$  and  $p = 3$ . For  $p = 1$  the effect of finite-lattice size is quite small below  $T_c$  and above  $T_c$  substantial "finite-size tails" are present. For  $p = 3$  finite-size

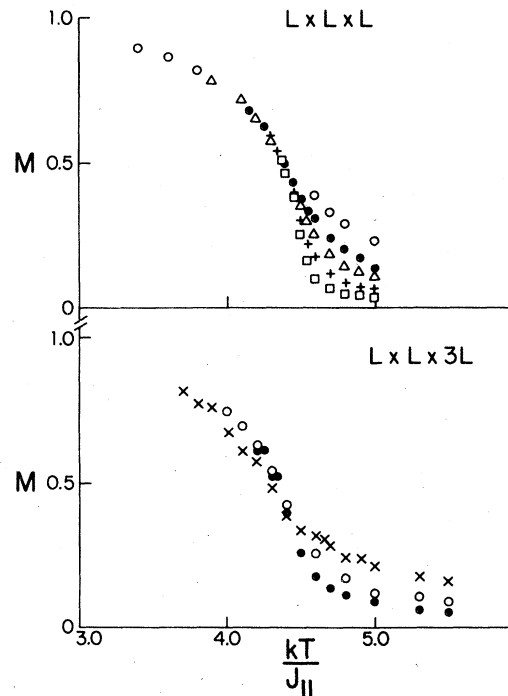


FIG. 2. Temperature dependence of the order parameter (spontaneous magnetization) for two different sample shapes for  $\Delta = 1.0$ . Data are shown for:  $L = 4, x$ ;  $L = 6, \circ$ ;  $L = 8, \bullet$ ;  $L = 10, \Delta$ ;  $L = 14, +$ ;  $L = 20, \square$ .

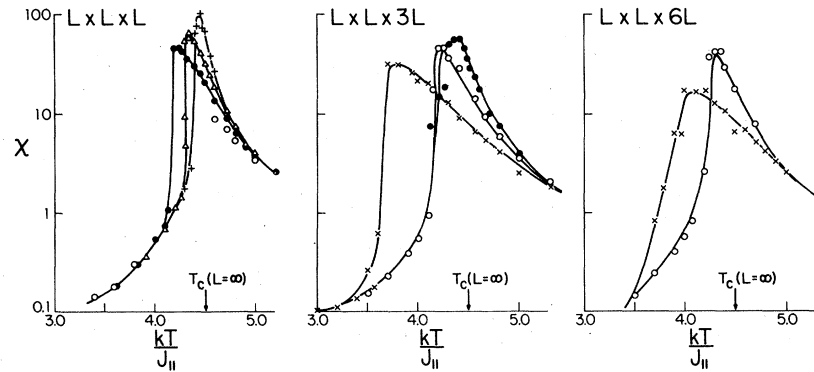


FIG. 3. Temperature dependence of the susceptibility for different sample shapes for  $\Delta = 1.0$ . Data are shown for:  $L = 4, x$ ;  $L = 6, \circ$ ;  $L = 8, \bullet$ ;  $L = 10, \Delta$ ;  $L = 14, +$ .

effects are evident well below  $T_c$  as well as at high temperatures.

The finite-size behavior of the magnetic susceptibility is shown for several  $p$  values in Fig. 3. Here too the peak position varies much more rapidly with lattice size for increasing  $p$  values.

#### B. $\Delta < 1.0$

Typical data for  $\Delta = 0.1$  are shown in Figs. 4–6. In Fig. 4 specific-heat results are plotted for several lattice sizes and three different sample shapes. For  $\Delta = 0.1$  the effects of finite-lattice size are much more pronounced for  $p = 1$  than for larger  $p$ . This is true for both the location and the maximum value of the specific-heat curve. For comparison we have also plotted the exact specific-heat curve for an isolated Ising chain (i.e., the one-dimensional Ising model).

Even though the *intra-chain* interactions are an order of magnitude larger than the *inter-chain* coupling, the region of pseudo-one-dimensional behavior is restricted to very high temperature. Data for the spontaneous magnetization for  $\Delta = 0.1$  are shown in Fig. 5. Finite-size effects are pronounced both below as well as above the transition temperature for  $p = 1$  but for  $p = 3$  virtually no size dependence is evident below  $T_c$ . Since the one-dimensional Ising model does not order, no comparison is possible for the order parameter. The behavior of the magnetic susceptibility, shown in Fig. 6 is qualitatively similar to that of the specific heat. In particular the peak position is much more size dependent for  $p = 1$  than for larger  $p$ . Here too the susceptibility approaches the pure one-dimensional curve only at quite high temperature.

The general characteristics of the data taken for

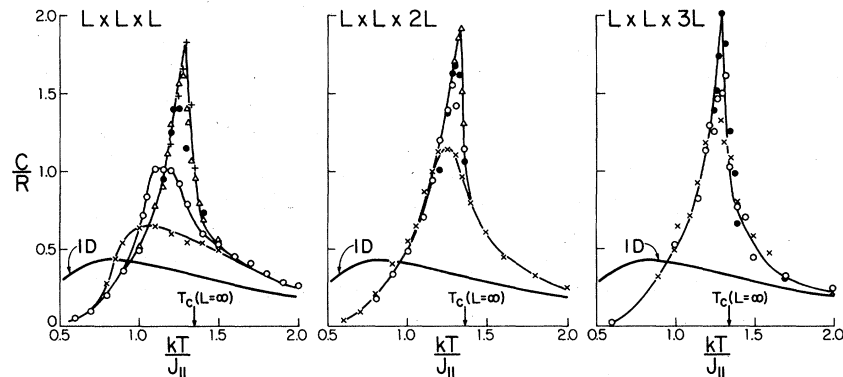


FIG. 4. Temperature dependence of the specific heat for different sample shapes with  $\Delta = 0.1$ . Data are shown for:  $L = 4, x$ ;  $L = 6, \circ$ ;  $L = 8, \bullet$ ;  $L = 10, \Delta$ ;  $L = 14, +$ . The heavy curves labeled 1D shows the exact behavior for an Ising chain with nearest-neighbor coupling  $J_{||}$ .

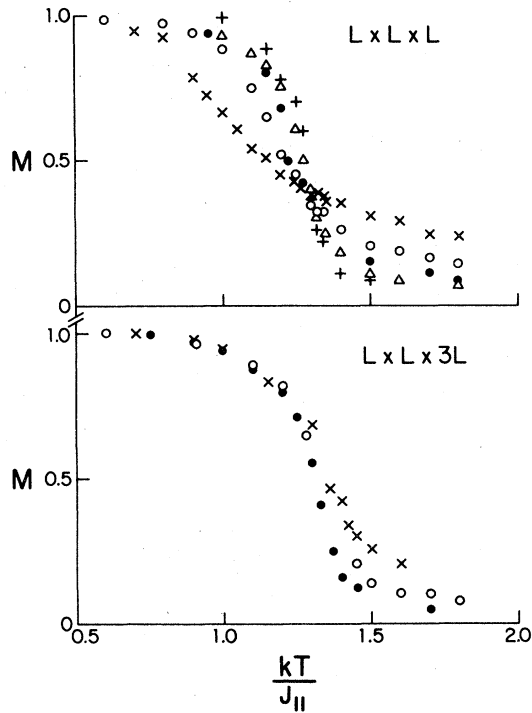


FIG. 5. Temperature dependence of the order parameter (spontaneous magnetization) for two sample shapes with  $\Delta=0.1$ . Data are shown for:  $L=4$ ,  $x$ ;  $L=6$ ,  $o$ ;  $L=8$ ,  $\bullet$ ;  $L=10$ ,  $\Delta$ ;  $L=14$ ,  $+$ .

other  $\Delta$  values were quite similar. As the interactions become more spatially anisotropic finite-size effects become increasingly pronounced for small  $p$ . As  $\Delta$  is decreased the resultant behavior does become more one-dimensional in character. This effect will be explored in more detail in the following section.

## IV. ANALYSIS AND DISCUSSION

### A. Finite-size behavior

The predicted variation in pseudo-critical temperature [see Eq. (8)] was tested using several different "effective sizes"  $\bar{L}$  [see Eq. (11)]. In Fig. 7 we show the size dependence of  $T_c^L$  with  $\bar{L}$  defined by Eq. (11a) for several system shapes for  $\Delta=1.0$  and  $\Delta=0.1$ . For  $\Delta=1.0$  the least finite-size variation occurs for  $p=1$  but for  $\Delta=0.1$  the greatest variation occurs for  $p=1$ . This tendency became even more pronounced for small values of  $\Delta$ .

Finite-size scaling was also tested for the thermodynamic properties. In Fig. 8 we show finite-size scaling plots for the order parameter for  $\Delta=0.1$ , and in Fig. 9 we show corresponding plots for the high-temperature susceptibility. Finite-size effects are so pronounced for  $p=1$  that the magnetization data simply do not collapse onto a single curve. In contrast the scaling behavior is quite good for  $p=2$  and 3. The scaling behavior of the high-temperature susceptibility for  $\Delta=0.1$  is equally good for all three  $p$  values (see Fig. 9).

### B. Crossover from 3D to 1D behavior

As  $\Delta$  decreases the thermodynamic properties of the model become more and more 1D in character. In Fig. 10(a) we show the temperature dependence of the specific heat for a wide range of  $\Delta$ . The specific heat does not show 1D behavior for  $\Delta > 0.1$ . At the smallest  $\Delta$  value ( $\Delta=0.003$ ) the data show no distinct peak and are essentially identical to the 1D curve down to  $kT/J_{||} \sim 0.4$  below which the data fall well below the 1D curve. In Fig. 10(b) we show the specific heat for a two-dimensional Ising model with anisotropic NN coupling.<sup>6,14</sup> The behavior is qualitatively the same for  $d=2$  and 3; however, the

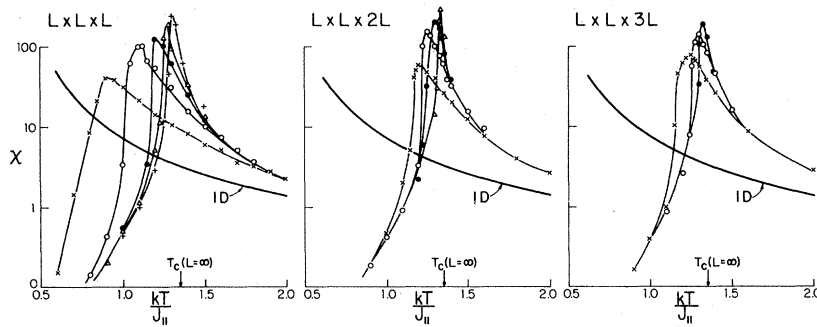


FIG. 6. Temperature dependence of the susceptibility for different sample shapes with  $\Delta=0.1$ . Data are shown for:  $L=4$ ,  $x$ ;  $L=6$ ,  $o$ ;  $L=8$ ,  $\bullet$ ;  $L=10$ ,  $\Delta$ ;  $L=14$ ,  $+$ . The heavy curve labeled 1D shows the exact behavior for an Ising chain with nearest-neighbor coupling  $J_{||}$ .

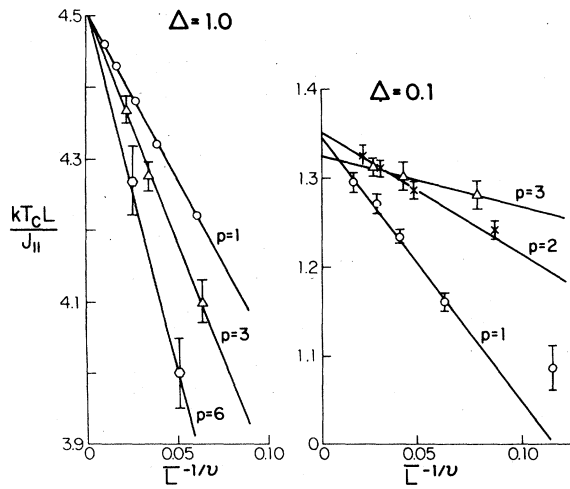


FIG. 7. Finite-size behavior of the pseudo-critical temperature  $T_c^L$  for different sample shapes.

specific-heat peak is more symmetric and  $T_c$  is lower for  $d=2$  than for  $d=3$  and the approach to 1D behavior is slightly more rapid as  $\Delta \rightarrow 0$ . The entropy was determined from integration of the specific heat:

$$S(T) = \int_0^T \frac{C}{T} dT' \quad (12)$$

The behavior of the internal energy, Fig. 11, and entropy, Fig. 12, are quite similar and show the increasing 1D character of the model as  $\Delta$  becomes smaller. The susceptibility, plotted in Fig. 13, also becomes increasingly 1D as  $\Delta$  decreases. The high-temperature series estimate for  $\Delta=0.01$  is generally in good agreement with our result.

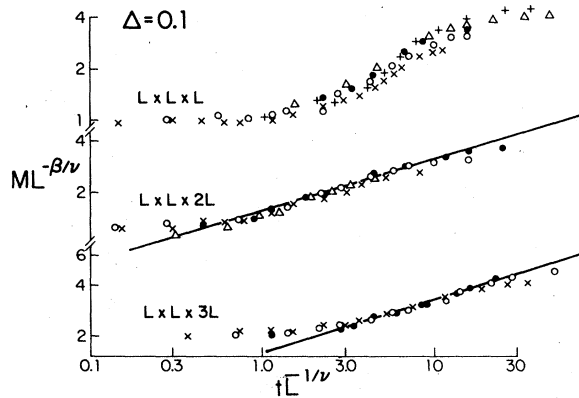


FIG. 8. Finite-size scaling plot for the order parameter for different sample shapes with  $\Delta=0.1$ . Data are shown for:  $L=4, x$ ;  $L=6, \circ$ ;  $L=8, \bullet$ ;  $L=10, \Delta$ ;  $L=14, +$ .

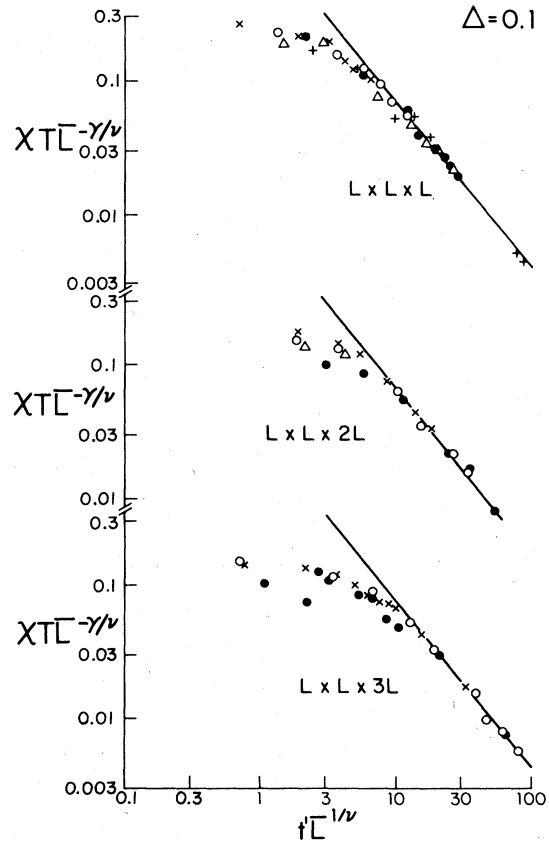


FIG. 9. Finite-size scaling plot for the susceptibility for different sample shapes with  $\Delta=0.1$ . Data are shown for  $L=4, x$ ;  $L=6, \circ$ ;  $L=8, \bullet$ ;  $L=10, \Delta$ ;  $L=14, +$ .

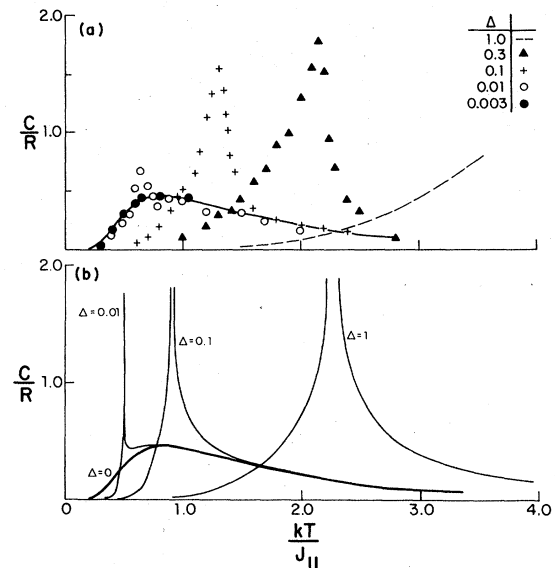


FIG. 10. (a) Specific heat vs temperature for various values of  $\Delta$  for the simple cubic lattice. The solid curve shows the behavior of the 1D Ising model. (b) Specific heat vs temperature for various values of  $\Delta$  for the square lattice (see Refs. 14 and 6).

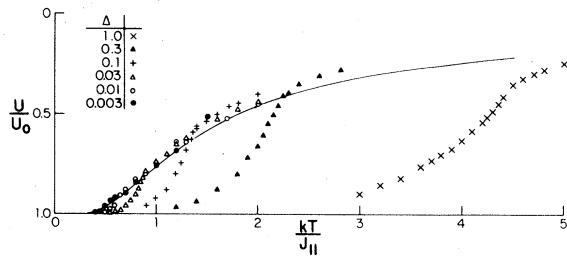


FIG. 11. Temperature variation of the internal energy for several  $\Delta$  values. Data points show extrapolated infinite lattice estimates. The solid curve shows the 1D Ising model behavior.

The behavior of the spontaneous magnetization with  $\Delta$  is uninteresting. As  $\Delta$  is decreased the temperature at which  $M$  begins to drop also goes down but neither the shape nor critical amplitude change.

The variation of  $T_c$  with  $\Delta$  is shown in Fig. 14. These data show that neither mean-field theory nor modified-mean-field theory [Eq. (2)] are accurate anywhere within the range of  $\Delta$  studied. As  $\Delta \rightarrow 0$  the modified mean-field theory becomes asymptotically exact, but our results show that *extremely* small values of  $\Delta$  are needed in order to enter the asymptotic region. The series estimates, however, agree well with our values. The asymptotic exact form [Eq. (3)], remains accurate to surprisingly large values of  $\Delta$  where the system has little 1D character.

C. Critical behavior

We have used finite-size scaling theory to analyze the critical behavior for  $0.01 \leq \Delta \leq 1$ . In all cases the

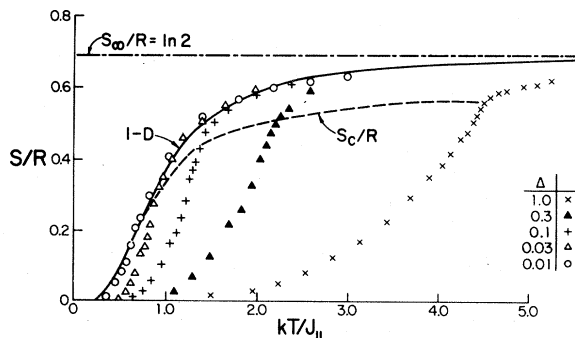


FIG. 12. Temperature variation of the entropy for several  $\Delta$  values. Data points show extrapolated infinite-lattice estimates. The solid curve shows the 1D Ising model behavior. The dashed line shows the variation of the critical entropy.

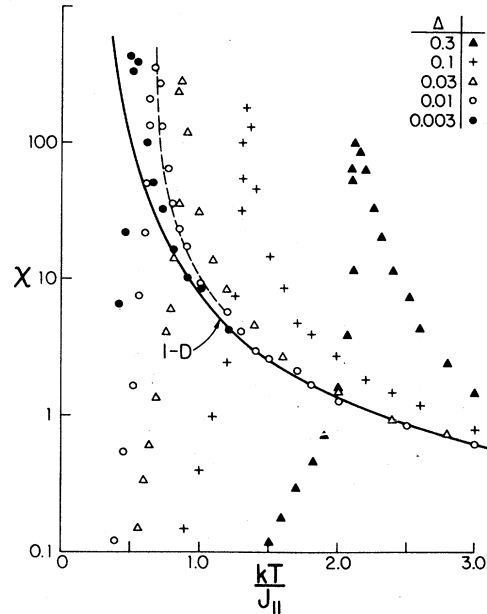


FIG. 13. Temperature variation of the susceptibility for several  $\Delta$  values. Data points show extrapolated infinite-lattice estimates. The solid curve shows the 1D Ising model behavior. The dashed curve is the result from a high-temperature series-expansion calculation (see Refs. 5 and 6) for  $\Delta = 0.01$ .

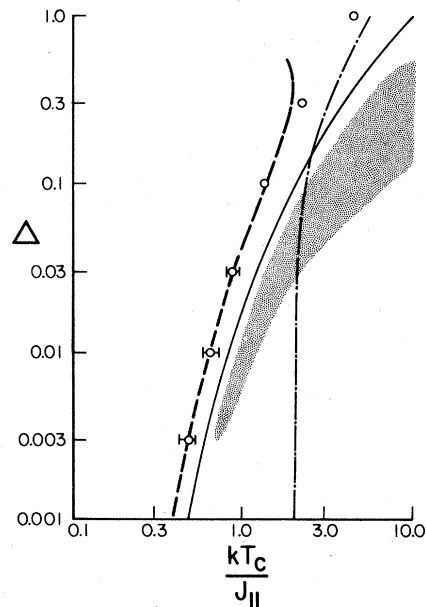


FIG. 14. Dependence of the critical temperature  $T_c$  on  $\Delta$ . Circles are Monte Carlo values and the dashed line is the exact asymptotic result (Ref. 7). The dot-dash curve is the mean-field result and the solid curve is the result of the modified mean-field theory prediction of Ref. 4. The stippled area shows the approximate crossover region from 3D critical behavior to 1D behavior.

TABLE I. Results of using finite-size scaling theory to analyze the critical amplitudes for  $0.01 \leq \Delta \leq 1.0$ .

| $\Delta$ | $B$             | $E^+$           | $b$            | $A^-$          | $A^+$           | $A^-/A^+$      | $R = \frac{A^+E^+}{B^2}$ |
|----------|-----------------|-----------------|----------------|----------------|-----------------|----------------|--------------------------|
| 1.0      | 1.57            | 1.058           | $-2.2 \pm 1.0$ | $2.8 \pm 0.6$  | $2.1 \pm 0.6$   | $1.3 \pm 0.5$  | $0.90 \pm 0.30$          |
| 0.3      | $1.55 \pm 0.05$ | $1.18 \pm 0.10$ | $-1.8 \pm 0.6$ | $2.4 \pm 0.5$  | $1.8 \pm 0.5$   | $1.3 \pm 0.45$ | $0.66 \pm 0.30$          |
| 0.1      | $1.55 \pm 0.05$ | $1.32 \pm 0.10$ | $-1.2 \pm 0.4$ | $1.8 \pm 0.5$  | $1.3 \pm 0.3$   | $1.4 \pm 0.5$  | $0.71 \pm 0.25$          |
| 0.03     | $1.6 \pm 0.2$   | $2.0 \pm 0.2$   | $-0.6 \pm 0.2$ | $1.2 \pm 0.3$  | $0.95 \pm 0.2$  | $1.3 \pm 0.4$  | $0.74 \pm 0.32$          |
| 0.01     | $1.6 \pm 0.2$   | $3.2 \pm 0.2$   | $-0.4 \pm 0.2$ | $0.85 \pm 0.2$ | $0.75 \pm 0.15$ | $1.1 \pm 0.35$ | $0.94 \pm 0.36$          |

exponents were consistent with the expected 3D Ising values. The data were not sufficiently accurate to allow a truly rigorous test of exponent values, however, assuming Ising values we could obtain rather accurate estimates for critical amplitudes. The specific-heat amplitudes were the least accurate because of the uncertainty in the background term [see Eq. (10d)]. The results are shown in Table I. The susceptibility amplitude  $E^+$  increases as  $\Delta \rightarrow 0$  while the specific-heat amplitudes  $A^+$  decrease. The order parameter amplitude remains relatively constant. We have also determined the "universal" amplitude<sup>15</sup>  $R = A^+E^+/B^2$  (see Table I). Within the admittedly large errors  $R$  is indeed independent of  $\Delta$ . We add a word of caution because the finite-size scaling analysis for  $\Delta = 1$  misestimates the background term  $b$  and hence seriously overestimates  $A^+$ .

#### D. Comparison with experiment

One of the most one-dimensional physical systems known is  $\text{CoCl}_2 \cdot 2\text{NC}_5\text{H}_5$ . Experimental specific-heat data are shown in Fig. 15 along with series expansion<sup>6</sup> and Monte Carlo results for  $\Delta = 0.01$ . The series results lies slightly too high at high temperatures and is too low at low temperatures. The Monte Carlo curve agrees rather well over a wide temperature range but is noticeably too high near  $T_c$ . We do not know if the discrepancy is due to errors in our data, the experimental data, or to the inadequacy of the model. For  $\text{CoCl}_2 \cdot 2\text{H}_2\text{O}$  series expansions agree quite well with the experimental data assuming  $\Delta = 0.2$ . Interpolation between our data for  $\Delta = 0.1$  and 0.3 support this conclusion. Experimental measurements<sup>17,18</sup> of the specific heat of  $\text{CsCoCl}_3 \cdot 2\text{H}_2\text{O}$  show two clearly separated peaks. The rounded, higher temperature maximum corresponds to Ising

linear chain behavior with  $J_{||} = 19$  K. A sharp peak at 3.38 K signals the onset of 3D long-range order. The ratio  $kT_c/J_{||} \approx 0.18$  is clearly in the asymptotic region where Eq. (3) is valid and corresponds to a value of  $\Delta \sim 10^{-6}$ . Estimates for the interchain interactions obtained from the magnetic phase boundaries are of the order of  $\Delta \sim 10^{-2}$ . It is believed that the nearest-neighbor intrachain coupling includes a substantial Dzyaloshinski-Moriya term<sup>17</sup> and that the interchain interactions may be almost isotropic. If these expectations are valid, the true Hamiltonian

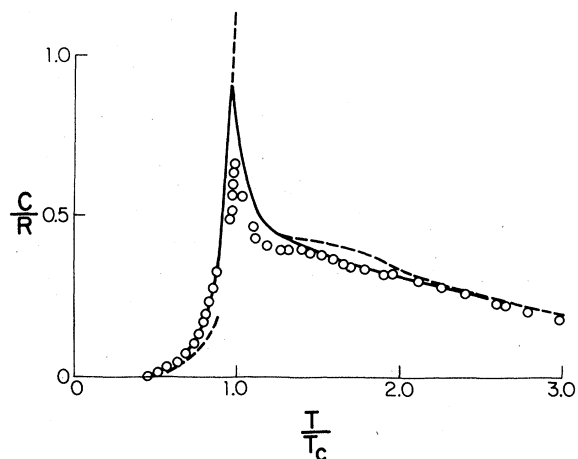


FIG. 15. Comparison between the experimental specific-heat results for  $\text{CoCl}_2 \cdot 2\text{NC}_5\text{H}_5$  shown by open circles (see Ref. 16) and the Monte Carlo result for  $\Delta = 0.01$  given by the solid curve. The dashed curves were derived from high- and low-temperature series expansions (Ref. 6).



is sufficiently different from Eq. (1) that Eq. (3) is probably not valid.

### V. CONCLUSIONS

We find that the crossover from 3D to 1D behavior occurs quite slowly and smoothly. Finite-size effects are very simple shape dependent for all  $\Delta$ . An analysis of the critical behavior has enabled us

to determine critical amplitudes and check the universality of the ratio  $R = A^+E^+/B^2$ .

### ACKNOWLEDGMENTS

This research was supported in part by the National Science Foundation. We also wish to thank Professor Y. Imry, Dr. M. A. Novotny, and Dr. E. B. Rasmusen for helpful comments.

- 
- <sup>1</sup>See, e.g., C. Domb, in *Phase Transitions and Critical Phenomena*, edited by C. Domb and M. S. Green (Academic, New York, 1974), Vol. 3.
- <sup>2</sup>For a review of work on real anisotropic systems see W. P. Wolf, *J. Phys. (Paris) Suppl.* **32**, C1 (1971).
- <sup>3</sup>See, e.g., L. J. de Jongh, *J. Appl. Phys.* **49**, 1305 (1978).
- <sup>4</sup>J. W. Stout and R. C. Chisholm, *J. Chem. Phys.* **3C**, 979 (1962); D. Hone, P. A. Montano, and T. T. Tonegawa, *Phys. Rev. B* **12**, 5141 (1975); H. Sato, *J. Phys. Chem. Solids* **19**, 54 (1961).
- <sup>5</sup>M. F. Sykes, D. L. Hunter, D. S. McKenzie, and B. R. Heap, *J. Phys. A* **5**, 667 (1972); M. F. Sykes, D. S. Gaunt, J. W. Essam, and C. J. Elliot, *ibid.* **6**, 1507 (1973).
- <sup>6</sup>R. Navarro and L. de Jongh, *Physica* **94 B and C**, 67 (1978).
- <sup>7</sup>C. Y. Weng, R. B. Griffiths, and M. E. Fisher, *Phys. Rev.* **162**, 475 (1967); M. E. Fisher, *ibid.* **162**, 480 (1967).
- <sup>8</sup>D. P. Landau, *Phys. Rev. B* **13**, 2997 (1976). An excellent review of importance sampling Monte Carlo methods may be found in K. Binder, in *Monte Carlo Methods in Statistical Physics*, edited by K. Binder (Springer Verlag, Berlin, 1979), Chap. 1.
- <sup>9</sup>A. B. Bortz, M. H. Kalos, and J. L. Lebowitz, *J. Comput. Phys.* **17**, 10 (1975).
- <sup>10</sup>Tom Graim, M.S. thesis (University of Georgia, 1978) (unpublished).
- <sup>11</sup>M. E. Fisher, in *Proceedings of the International Summer School Enrico Fermi, Course 51, Varenna, 1970*, edited by M. S. Green (Academic, New York, 1971).
- <sup>12</sup>D. P. Landau, *Phys. Rev. B* **14**, 255 (1976).
- <sup>13</sup>A. E. Ferdinand and M. E. Fisher, *Phys. Rev.* **185**, 832 (1969).
- <sup>14</sup>L. Onsager, *Phys. Rev.* **65**, 117 (1944).
- <sup>15</sup>A. Aharony and P. C. Hohenberg, *Phys. Rev. B* **13**, 3081 (1976).
- <sup>16</sup>K. Takeda, S. Matsukawa, and T. Haseda, *J. Phys. Soc. Jpn.* **30**, 1330 (1971).
- <sup>17</sup>A. Heweijer, W. J. M. de Jonge, A. C. Botterman, A. L. M. Bongaarts, and J. A. Cowen, *Phys. Rev. B* **5**, 4618 (1972).
- <sup>18</sup>K. Kopinga, Q. A. G. van Vlimmeren, A. L. M. Bongaarts, and W. J. M. de Jonge, *Physica* **86-88B**, 671 (1977).